Rojas-Lema, SP.; Lascano-Aimacaña, DS.; Ivorra-Martínez, J.; Gómez-Caturla, J.; Balart, R.; Garcia-Garcia, D. (2021). Manufacturing and Characterization of High-Density Polyethylene Composites with Active Fillers from Persimmon Peel Flour with Improved Antioxidant Activity and Hydrophobicity. Macromolecular Materials and Engineering. 306(11):1-16. https://doi.org/10.1002/mame.202100430

Manufacturing and Characterization of High-Density Polyethylene Composites with Active Fillers from Persimmon Peel Flour with Improved Antioxidant Activity and Hydrophobicity

Sandra Rojas-Lema[1,2], Diego Lascano *[1,2], Juan Ivorra-Martinez[1], Jaume Gomez-Caturla[1], Rafael Balart[1], Daniel Garcia-Garcia[1]

[1] Technological Institute of Materials (ITM), Universitat Politècnica de València (UPV), Plaza Ferrándiz y Carbonell 1, 03801 Alcoy, Spain.
[2] Escuela Politécnica Nacional, 17-01-2759, Quito, Ecuador; dielas@epsa.upv.es (D.L)
* Correspondence: dielas@epsa.upv.es

Abstract: This study shows the potential of persimmon peel waste (PPF) as renewable active filler in bio-based polyethylene composites, with improved antioxidant properties and resistance to water uptake. To improve the interaction between the hydrophilic biofiller and the highly hydrophobic matrix, several compatibilization approaches were assessed. The first approach consisted of using a polyethylene grafted copolymer with maleic anhydride (PE-*g*-MA). The second approach consisted of modifying the PPF surface with two treatments before compounding with Bio-HDPE. The first consisted on conventional silanization with (3-glycidyloxypropyl)trimethoxysilane, while the second consisted on esterification with palmitoyl chloride. The results showed an improvement of the matrix/biofiller interaction, as observed by FESEM, leading to an increase in Young's modulus of 10% in composites compatibilized with PE-*g*-MA, and silanized PPF compared to composites without compatibilizer and no surface treatment on PPF. Interestingly, treatment with palmitoyl chloride led to an increase in the hydrophobic behavior of composites keeping the water contact angle virtually constant at 128º. This effect was also reflected in a clear decrease in water absorption capacity of only 0.3 wt.% over 9 weeks. Finally, PPF increased stabilization against oxidation, improving the oxidation induction time from 4.8 min (Bio-HDPE) to 82.5 min for composites with silanized PPF.

Keywords: Bio Polyethylene; revalorization residues; natural fillers; compatibilization; Persimmon peel.

1. Introduction

The trend to incorporate fruits and vegetables of high nutritional value as a fundamental basis in people's daily diet has increased considerably in recent years [1]. Several studies have demonstrated that they can help in the prevention and treatment of degenerative diseases, largely due to the large number of active compounds with antioxidant properties [2-4]. This has led to a remarkable growth in consumption and production of the persimmon fruit in different countries and regions, including Europe, which is the world's second-largest producer with 8.5% market share, behind China (87.6%), between 2015 and 2019 according to the Food and Agriculture Organization of the United Nations [5]. The popularity of this fruit is due to the great benefits it brings to people's health, since it is a food with a great source of dietary fiber, tannins, vitamin C, phenolic compounds, among others, besides having a low content of saturated fats and calories [6, 7]. This has triggered an increase in its consumption and industrialization, where the flesh is preferred for the preparation of juices, jams, ice cream, among others [8-10]. As a result, a large amount of waste is generated from the peel, calyx, and seeds. Several alternatives have been proposed to take advantage of these wastes since they are rich in valuable compounds. In this regard, persimmon peel has attracted attention because it can serve as a source of active compounds, due to its high carotenoids, polyphenols and proanthocyanidins content, which have a great antioxidant effect [8]. Another feasible approach for the valorization of agro-industrial and food wastes is the production of the so called wood-plastic composites (WPC), or more accurately, natural fiber reinforced plastics (NFRP) which aim obtaining environmentally friendly composites by combining a polymeric matrix (thermosetting or thermoplastic) and natural fillers (usually lignocellulosic materials) in the form of particles, fibers or fine powders to give a series of wood-like materials with balanced properties. In addition to minimizing the environmental impact of industrial wastes, the use of these lignocellulosic fillers has a positive effect on reducing the overall production costs, and can contribute to more sustainable materials [11, 12].

Currently, commodity thermoplastic materials such as polypropylene (PP) and polyethylene (PE) top the list of the most commonly used materials for WPC manufacturing due to the ease of processing by conventional methods, and good final properties such as flexibility, good chemical resistance and lightness, among others [13]. This has placed high-density polyethylene (HDPE) as the third most used material in the European market, with a share of 12.4% [14]. This has raised concerns about the uncontrolled use of petroleum-derived materials, which has triggered the search for new biomaterials to replace the current ones [15].

To this end, recent research is being focused on developing polymers from renewable resources. Polyethylene can be obtained from renewable resources by the polymerization of ethylene monomer derived from the catalytic dehydration of bioethanol from sugarcane [16]. This biobased polyethylene has identical properties to those of its petrochemical counterpart.

One of the main drawbacks in the manufacture of wood-plastic composites or polymers filled with lignocellulosic particles, is the poor compatibility between the thermoplastic matrix and the natural fillers, due to the difference in polarity. Lignocellulosic fillers are highly hydrophilic due to the large number of hydroxyl groups present in their structure, which can also favor aggregates formation, while polymeric matrices usually are highly hydrophobic. This difference results in composites with poor mechanical properties since loads cannot be appropriately transferred between the lignocellulosic filler and the surrounding matrix [17]. To this end, many research studies have focused on assessing the usefulness of different types of strategies to improve the interaction between these two components. These techniques include the use of compatibilizers such as graft copolymers, which act as a bridge between the matrix and the biofiller, thus enhancing their interaction [18, 19]. Polyethylene grafted with maleic anhydride (PE-*g*-MA) is one of the most widely used compatibilizers in WPC with polyethylene matrices due to its dual functionality that can interact with both the polyethylene matrix (polyethylene segment chains in PE-*g*-MA), and the lignocellulosic filler (by the interaction of maleic anhydride with hydroxyl groups in lignocellulosic filler). Garcia-Garcia [20], studied the effect of different types of maleic anhydride-based compatibilizers, namely polyethylene-*graft*-maleic anhydride (PE-*g*-MA), polypropylene-*graft*-maleic anhydride (PP-*g*-MA), and polystyrene-block-poly(ethylene-*ran*-butylene)-*block*-polystyrene-*graft*-maleic anhydride (SEBS-*g*-MA), on the compatibility of bio-based polyethylene composites reinforced with peanut shell flour. Scanning electron microscopy images revealed that the use of these compatibilizers enhanced the interaction between the peanut shell flour and the surrounding matrix, leading to an improvement in its tensile properties. The dual functionality of these copolymers causes the anhydride groups to react with the hydroxyl (-OH) groups available in the biofiller to form ester groups and, on the other hand, the polyethylene segments of these copolymers can rearrange to interact with the polyethylene matrix, thus helping to improve their interaction and dispersion.

Another strategy to improve the compatibility between the reinforcement and the matrix in WPCs or NFRP is to carry out surface treatments on the fillers with the main aim of blocking the hydroxyl groups with the subsequent decrease in hydrophilicity. Several surface treatments

such as mercerization, silanization, esterification, among others, have proven to be very effective in reducing the hydrophilic nature of biofillers [13, 21-23]. The modification of the biofillers by alkoxy silanes leads to a strong interaction between the hydroxyl (-OH) groups contained in the biofillers with the hydrolyzed alkoxy groups, which give silanol groups (-Si-OH) [24]. In addition, it has been shown that esterification of the hydroxyl groups of the biofillers by treatment with fatty acids or their salts, such as palmitoyl chloride or with anhydrides such as acetic anhydride, positively contributes to increase their hydrophobic behavior, thus increasing their affinity with the highly hydrophobic matrices. Bijaisoradat, Yue [25], improved the hydrophobic nature of wood flour (WF) in recycled polyethylene composite materials, by two different surface treatments, namely silanization with propyltrimethoxysilane and esterification with acetic anhydride. Both processes led to a remarkable improvement on filler dispersion and compatibility. Moreover, both surface treatments improved the mechanical properties and thermal stability of the obtained composite materials. Dominici, García García [26], investigated the effect of surface treatments, such as alkali bleaching and palmitoyl chloride esterification, on overall properties of bio-based polyethylene composites and coffee silverskin. In addition, reactive graft copolymerization with maleic anhydride was performed for the alkali treated samples to improve their compatibility with the matrix. They reported a remarkable increase in the hydrophobic nature of the coffee silverskin particles treated with palmitoyl chloride, leading to a water absorption of barely 0.2 wt.% compared to 0.7 wt.% of untreated coffee silverskin particles after an immersion period of one-month.

The purpose of this work is to develop high environmentally friendly lignocellulosic particle-filled polymer composites with biobased high-density polyethylene (Bio-HDPE) matrix and an active biofiller from persimmon peel flour (PPF). In this study, two different strategies are proposed to improve polymer-filler interaction. The first approach considers the use of a graft copolymer compatibilizer, namely polyethylene-*graft*-maleic anhydride (PE-*g*-MA), while a second strategy consists of two different surface treatments of PPF with (3-glycidyloxypropyl)trimethoxysilane or with palmitoyl chloride. The effect of these different compatibilizing strategies on mechanical properties (tensile, impact strength and hardness), dynamic-mechanical thermal behaviour (DMTA), morphology, thermal and color properties of Bio-HDPE/PPF composites with a constant PPF loading of 20 wt.% was carried out. The effect of different surface treatments on the wetting properties of PPF was also evaluated by dynamic contact angle and water uptake characterization. Finally, the antioxidant effect of PPF phenolic

compounds on Bio-HDPE/PPF composites was studied by (2,2-diphenyl-1-picryl-hydrazyl-hydrate) DPPH inhibition assay and oxidation induction time (OIT) at a constant temperature.

2. Experimental

2.1. Materials

A commercial biobased high-density polyethylene (Bio-HDPE) grade SHA7260 from Braskem and supplied by FKuR Kunststoff GmbH (Willich, Germany) was used as the polymer matrix. This Bio HDPE contains at least 94% biobased content and has a melt flow rate of 20 (g/10 min), and a density of 0.955 g/cm^3.

The filler was obtained from persimmon peel waste of the Spanish "Rojo Brillante" persimmon fruit (*Diospyros kaki*). Persimmon peel was micronized following several stages. The first stage consisted of washing with water to remove unwanted impurities (paper labels, dust, and so on). Next, the drying process was carried out in an oven at a constant temperature of 65 ºC for 5 days to remove moisture and flesh remains. Finally, the dried waste was ground in a Retsch Gmbh model ZM 1000 ultracentrifugal mill (Haan, Germany) with a sieve size of 250 µm and a rotation speed of 12,000 rpm. Persimmon peel flour (PPF) with particles of an average diameter of 60 - 125 µm was obtained, as shown in **Figure 1**. The total fiber, soluble fiber and insoluble fiber are 1.73, 0.82, and 0.87 g/100 g, respectively. In addition, the minerals present in persimmon peel are potassium (266 g/100 g), magnesium (12.7 g/100 g), sodium (4.49 g/100 g), manganese (0.23 g/100 g), iron (0.27 g/100 g), zinc (0.035 g/100 g), copper (0.03 g/100 g), and calcium (0.029 g/100 g) [27].

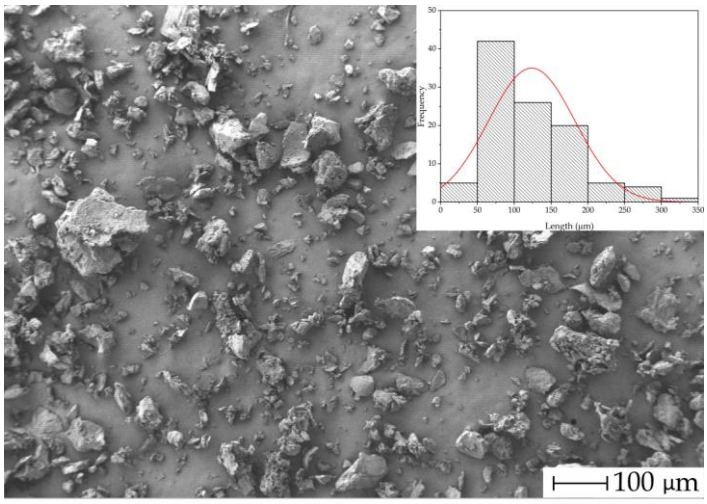

Figure 1. FESEM image of persimmon peel flour (PPF) particles at 50x with a marker scale of 100 μm.

The compatibilizer used was a polyethylene-*graft*-maleic-anhydride copolymer, (PE-*g*-MA) supplied by Sigma Aldrich (Madrid, Spain). This has an approximate amount of 0.5 wt.% maleic anhydride, a melting point T_m of 107 ºC, and a viscosity of 500 cP (at 140 ºC).

Persimmon peel flour (PPF) was subjected to two types of surface treatments. The first was based on a functionalization treatment with (3-glycidyloxypropyl)trimethoxysilane (GLYMO) supplied by Sigma Aldrich (Madrid, Spain), with a density of 1.07 g/cm^3 (at 25 ºC). The second surface treatment consisted of hydrophobization with palmitoyl chloride in the presence of 1,2 dichloroethane and pyridine, all provided by Sigma Aldrich (Madrid, Spain). The chemical structure of the PE-*g*-MA copolymer, as well as the two surface-modification compounds is shown in **Scheme 1**.

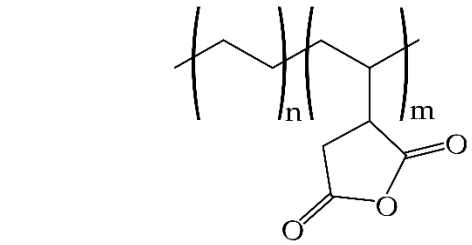

poly(ethylene-*graft*-maleic anhydride) - PE-*g*-MA

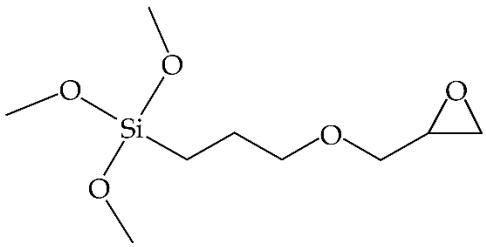

(3-glycidyloxypropyl)trimethoxysilane - GLYMO

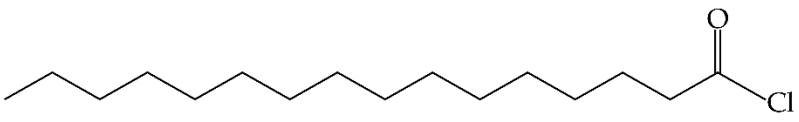

palmitoyl chloride

Scheme 1. Chemical structure of the maleic anhydride copolymer (PE-*g*-MA), and the two chemicals used to selectively modify the surface of persimmon peel flour.

2.2. Surface treatments on persimmon peel flour (PPF)

The PPF silanization process was carried out by immersing the flour particles in a solution of distilled water containing 1 wt.% GLYMO relative to the total PPF loading, as suggested by Quiles-Carrillo, Boronat [28]. The solution was stirred for 2 h at room temperature using a magnetic stirrer until a homogeneous solution was obtained. Then, the particles were removed, washed repeatedly with distilled water, and finally dried in an oven at a temperature of 80 °C for 12 h. **Scheme 2** shows a plot of the surface treatment of lignocellulosic particles by silanization. As it can be seen, esterification allows the silane to anchor into hydrophilic lignocellulose outer layer by a condensation reaction. In addition, the free silanols can react to form a polysiloxane layer [29].

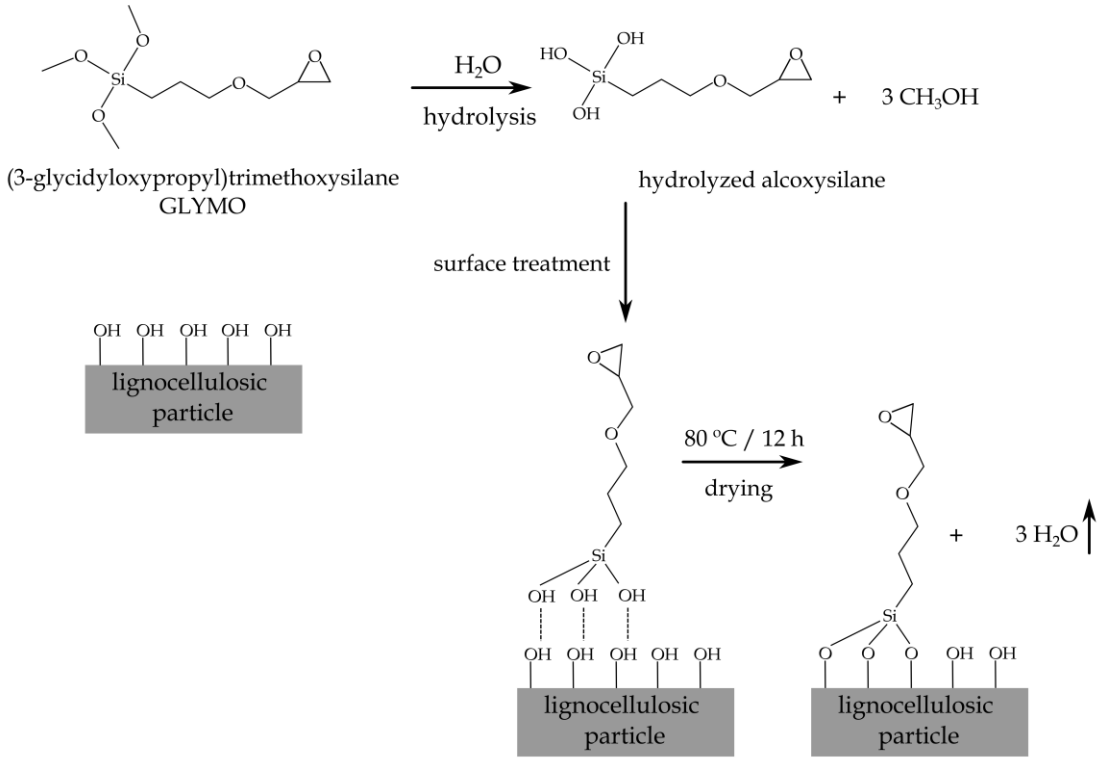

Scheme 2. Representation of the surface treatment of lignocellulosic particles from persimmon peel flour by silanization with GLYMO.

The hydrophobization treatment of PPF was carried out according to the procedure described by García-García, Carbonell [30]. Prior to treatment, the PPF was dried in an oven for 12 h at a temperature of 80 °C to prevent moisture absorption. In a three-necked round-bottomed flask containing a 130 mL solution of 1,2-dichloroethane and 5 g of the flour particles were introduced, stirred with a magnetic stirrer, and heated to 70 °C. Once the temperature was reached, 7 mL of pyridine was introduced under a nitrogen atmosphere, followed by the addition of 11 mL of palmitoyl chloride. Magnetic stirring and a constant temperature of 70 °C was maintained throughout the reaction time (90 min). The particles were then extracted and

washed with 1,2-dichloroethane and distilled water. Finally, the particles were dried at 80 °C for 12 h. This reaction allows the anchoring of a highly hydrophobic layer by blocking the hydroxyl groups contained in the lignocellulosic particles by esterification reactions, as shown in **Scheme 3** [31].

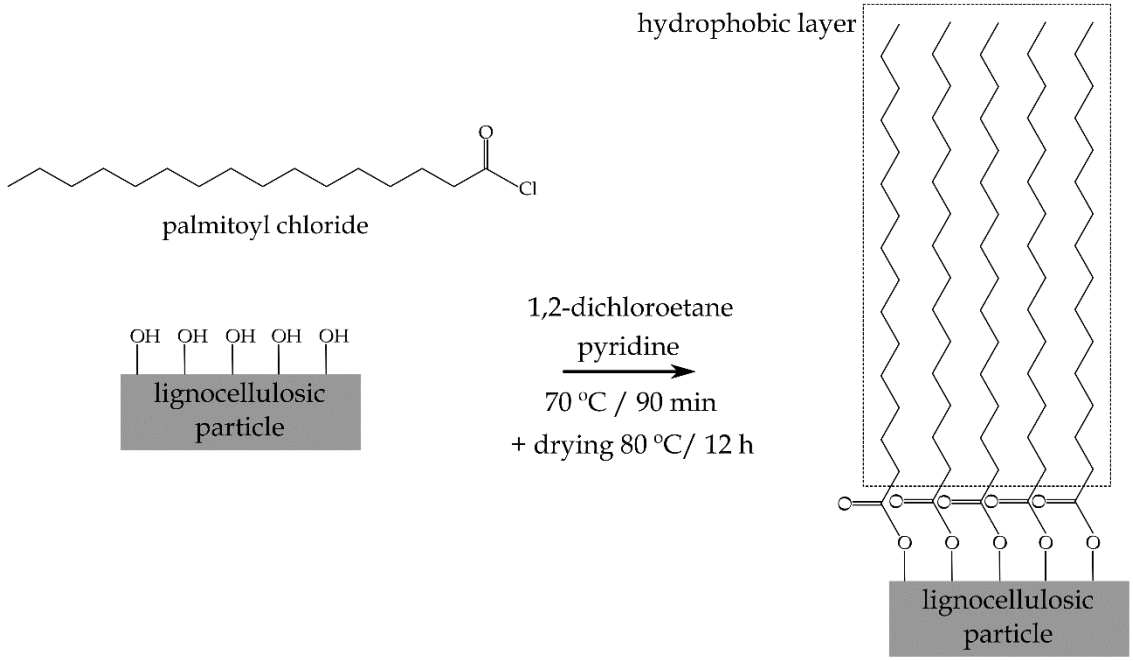

Scheme 3. Representation of the hydrophobic surface treatment of lignocellulosic particles from persimmon peel flour by using palmitoyl chloride.

The visual appearance of the PPF before and after the two surface treatments can be seen in **Figure 2**.

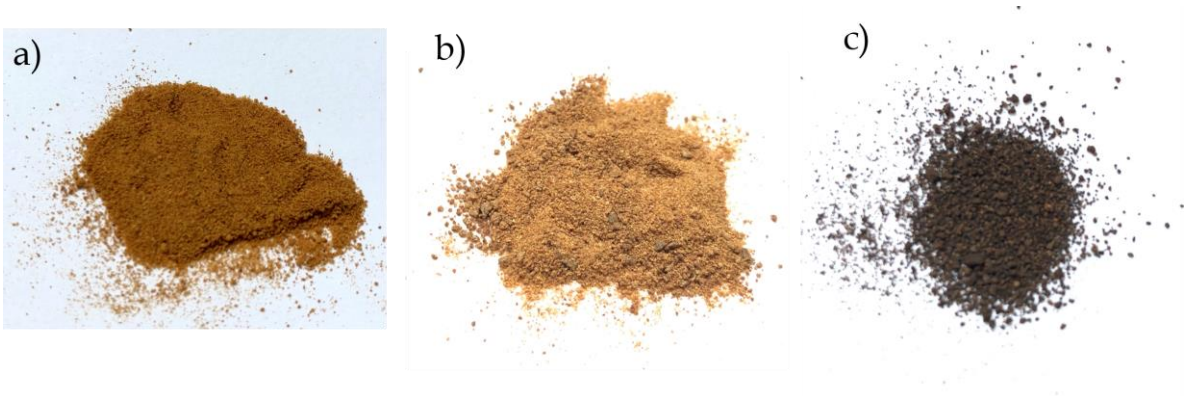

Figure 2. Photographs of a) untreated persimmon peel flour, b) persimmon peel flour after silanization with GLYMO treatment, and c) persimmon peel flour after hydrophobization treatment with palmitoyl chloride.

2.3. Manufacturing of Bio- HDPE/PPF composites

To remove the moisture content in the PPF (6 wt.% at 25 ºC), the PPF was subjected to a drying process in an oven at 65 °C for 12 h, prior to the manufacture of the composites. All formulations were first weighed and manually mixed in a ziplock bag prior to compounding by extrusion. All composites contained a constant PPF loading of 20 wt.%. As for the PE-*g*-MA formulation, 2 wt.% was used, and was directly mixed with the other components during the extrusion process. Samples were labeled with the code Bio-HDPE/PPF-XX, where XX stands for the compatibilization strategy: silanization with GLYMO (SI), compatibilization with polyethylene-*graft*-maleic (MA), and hydrophobization with palmitoyl chloride (PC). The extrusion process was carried out in a twin-screw co-rotating extruder from Dupra S.L. (Alicante, Spain). The temperature profile was set considering the maximum melting temperature of a conventional high-density polyethylene (HDPE), starting at the feed hopper, and ending at the nozzle with 135 - 140 - 145 - 150 ºC, and the rotation speed was set to 25 rpm. Once the filaments were collected, they were cooled down to room temperature, and pelletized in an air knife unit. To obtain standard specimens for tensile and Charpy impact tests, pellets of each formulation were molded on a Sprinter-11 Erinca S.L injection molding machine (Barcelona, Spain). The temperature profile was 140 ºC in the feed hopper, 150 ºC in the screw area and 160 ºC in the injection nozzle. The injection and cooling times were set at 5 and 30 s, respectively.

2.4. PPF characterization

2.4.1 Wettability

The wettability of treated and untreated PPF was characterized by dynamic contact angle using an Easy drop FM140 goniometer supplied by Krüss Equipments (Hamburg, Germany). The characterization was carried out at room temperature with distilled water droplets of approximately ~ 15 µL, and the dynamic water contact angle was measured at different times up to 120 s.

2.4.2. Morphological analysis

Morphological analysis of PPF particles was assessed by field emission scanning electron microscopy (FESEM). A Zeiss Ultra 55 FESEM microscope provided by Oxford Instruments (Abingdon, UK) was employed. An electron accelerating voltage of 1.5 kV was set. Prior to analysis, PPF particles were sputter-coated by applying an ultra-thin layer of gold-palladium in a EM MED20 high-vacuum sputter coater provided by Leica Microsystem (Milton Keynes, UK). The particle size was obtained using Image J Launcher v 1.41.

2.5. Bio-HDPE/PPF composites caracterization

2.5.1. Mechanical properties

The mechanical properties of neat Bio-HDPE and Bio-HDPE/PPF composites were analyzed by tensile, impact strength (Charpy) and hardness tests. Tensile tests were conducted on a ELIB 30 universal testing machine from Ibertest (Madrid, Spain); the test parameters and the dimensions of the dog-bone specimens were in accordance with ISO 527. A 5 kN load cell with a crosshead speed of 10 mm/min was used. The tensile modulus, E (MPa), tensile strength, σ_t (MPa), and elongation at break, ε_b (%) were measured by this test. At least 5 different specimens were tested and the corresponding tensile parameters were averaged.

The Charpy impact test was carried out to determine the impact strength. It was performed on a Charpy pendulum from Metrotec S.A. (San Sebastian, Spain) using a 1-J pendulum following ISO 179. The test was carried out on notched specimens ("V" notch type, 2 mm depth), and five specimens of each formulation were tested to obtain reliable data, showing the average value.

Shore D hardness was obtained at room temperature using a durometer model 673-D of J. Bot S.A. (Barcelona, Spain), following the guidelines of ISO 868, with a stabilization time of 15 s. This process was performed at five different points and averaged for all formulations.

2.5.2. Morphological characterization

Morphological analysis of the fractured surfaces of Bio-HDPE/PPF composites after impact testing was performed by field emission scanning electron microscopy (FESEM). A Zeiss Ultra 55 FESEM microscope provided by Oxford Instruments (Abingdon, UK) was employed. An electron accelerating voltage of 1.5 kV was used. Prior to analysis, sample surfaces were sputter-coated by applying an ultra-thin layer of gold-palladium in a model EM MED20 high-vacuum coater provided by Leica Microsystem (Milton Keynes, UK).

2.5.3 Thermal properties

Thermal characterization of Bio-HDPE and Bio-HDPE/PPF composites was carried out by differential scanning calorimetry (DSC). The DSC tests were conducted in an 821 DSC calorimeter from Mettler-Toledo Inc. (Schwerzenbach, Switzerland) with samples of approximately 5 – 8 mg. A dynamic thermal program was scheduled to obtain the main thermal transitions. This test consisted of three stages: an initial heating from 30 to 180 ºC was used to remove the thermal history derived from the manufacturing processes. This step was followed by a cooling cycle to -25 ºC. Finally, the samples were heated to 220 ºC. The heating and cooling

rate was set at 10 ºC/min, under a constant nitrogen atmosphere of 66 mL/min. The crystallization temperature was obtained from the cooling cycle, while the melting enthalpy and melting peak temperature were collected from the second heating cycle. The crystallinity percentage of each sample was obtained by **Equation 1.**

$$\chi_c = \frac{\Delta H_m}{\Delta H_m^0 \cdot (1 - w)} \cdot 100 \quad \% \tag{1}$$

Where ΔH_m^0 corresponds to the theoretical melting enthalpy of a fully crystalline HDPE (293 J/g) [26], ΔH_m stands for the melting enthalpy in (J/g), and *w* is the PPF weight fraction.

A second DSC test was carried out to analyze the effect of PPF on the oxidation induction time (OIT) of the Bio-HDPE matrix. This test consisted of two steps: the first one was a heating from 30 to 210 ºC at a heating rate of 5 ºC/min, followed by an isothermal step at a constant temperature of 210 ºC for 200 min; the test was carried out under air atmosphere to assess the effect of PPF on polymer oxidation.

The degradation and thermal stability at high temperatures of Bio-HDPE and its composites, as well as persimmon peel flour, were studied by thermogravimetric analysis (TGA) on a Linseis TGA1000 thermobalance (Selb, Germany), in standard alumina crucibles with a capacity of 70 µL. The weight of the different samples was maintained in a range between 15 - 20 mg. The samples were heated from 30 up to 800 ºC at a heating rate of 10 ºC/min under nitrogen atmosphere with a flow rate of 66 mL/min. The parameters obtained from the thermogravimetric curves were the onset temperature (T_{onset}), measured at 5% weight loss, and the temperature of maximum degradation rate (T_{deg}) extracted from the first derivative curve (DTG).

2.5.4. Dynamic-mechanical thermal analysis (DMTA)

The dynamic-mechanical thermal behaviour of Bio-HDPE and Bio-HDPE/PPF composites was evaluated by dynamic mechanical thermal analysis (DMTA). A dynamic analyzer model DMA1 from Mettler-Toledo (Schwerzenbach, Switzerland) was used; the system operates under cantilever/simple bending conditions. Rectangular specimens (20×7×1 mm^3) were subjected to a heating cycle ranging from -150 to 125 ºC with a heating rate of 2 ºC/min. The frequency and maximum flexural deflection were set to 1 Hz and 0.1%, respectively. The evolution of the storage modulus (*E'*) and the dynamic damping factor (tan δ) as a function of temperature was monitored throughout the test.

2.5.5. Color measurements

The effect of surface-treated PPF on the colour of Bio-HDPE/PPF composites was analyzed using a KONICA CM-3600d Colorflex-DIFF2 colorimeter from Hunter Associates Laboratory (Reston, Virginia, USA). The CIELab color scale (coordinates L^*, a^* and b^*) was collected, where L^* indicates brightness, a^* shows the range between red and green colors, and b^* shows the range between yellow and blue colors. The device was calibrated considering a standard white tile and a mirror unit for black. The total color difference (ΔE^*_{ab}) was determined by **Equation 2**:

$$\Delta E^*_{ab} = \sqrt{(\Delta L^*)^2 + (\Delta a^*)^2 + (\Delta b^*)^2} \quad (2)$$

Where ΔL^*, Δa^*, and Δb^* are the differences between the colour coordinates of the samples and the reference colour.

2.5.6. Water uptake analysis

The water absorption of Bio-HDPE and Bio-HDPE/PPF composites was studied in accordance to ISO 62:2008. Rectangular samples (80×10×4 mm^3) were immersed in distilled water for a period of 9 weeks. The test was performed at room temperature. The samples were extracted from the distilled water, dried with absorbent paper and weighed on an analytical balance model AG245 from Mettler-Toledo (Schwerzenbach, Switzerland) with an accuracy of 0.001 g. The samples then were immersed again in the distilled water. This process was repeated once per week on the same day during the test period. To ensure the accuracy of the data, all measurements were repeated in triplicate. The percentage of water absorption was obtained using **Equation 3**:

$$Water\ \ absorption = \frac{(W_t - W_0)}{W_0}\ \cdot 100\% \quad (3)$$

Where W_t is the weight of the dry sample in grams at any time t and W_0 is the weight of the initial dry sample in grams.

2.5.7. Antioxidant Measurement

The antioxidant effect of PPF phenolic compounds on Bio-HDPE/PPF composites was assessed by a 2,2-diphenyl-1-picrylhydrazyl radical (DPPH) inhibition test. DPPH is a stable nitrogenous organic radical that exhibits hydrogen acceptor capacity towards antioxidants. By means of spectrophotometry, the colour change that occurs during the reduction of the violet

colour of DPPH in a methanol solution due to the presence of antioxidant compounds was analyzed. A standard solution of 2,2-diphenyl-1-picrylhydrazyl supplied by Sigma Aldrich (Madrid, Spain) was prepared at 0.025 g/L in methanol (≥ 99.8 %) of HPLC grade supplied by Panreac Química (Barcelona, Spain) and placed in dark glass vials. Films of each sample weighing approximately 100 mg were prepared and immersed in 5 mL of the standard solution, giving a maximum antioxidant concentration of approximately 160 ppm. The vials containing the samples and a control (no sample) were closed and kept in light-free and shaking conditions for one week. The absorbance of the samples was recorded at 1, 24, 72 and 168 h, in triplicate, using an Agilent Technologies (Barcelona, Spain) Cary series UV-Vis-NIR spectrophotometer at 517 nm, where the unpaired electron of the free DPPH radical has the highest absorbance. The percentage inhibition of DPPH was calculated according to **Equation 4**:

$$DPPH_{inhibition} = \left(\frac{A_c - (A_s - A_b)}{A_c}\right) \cdot 100\% \quad (4)$$

Where A_c, A_s correspond to the absorbance of DPPH without sample and with samples, respectively. A_b stands for the absorbance of the samples in methanol without DPPH.

3. Results and discussion

3.1. Effect of surface treatment on wetting properties and morphology of PPF

3.1.1. Wettability

To investigate the effect of surface treatments on the wetting properties of persimmon peel flour, the evolution of the dynamic water contact angle over time was studied, as shown in **Figure 3** and **Figure 4**. As can be seen in **Figure 4** the reference value of contact angle (t=0) for the untreated PPF, silane-treated PPF and palmitoyl chloride-treated PPF is 112.4º, 118.5º and 128.6º, respectively. The evolution of the contact angle for the untreated PPF, shows a clear decrease with time due to its hydrophilic nature, reaching values close to 40º after 60 s and, while after 120 s, untreated PPF is completely wet with a contact angle below 30º, thus showing a highly hydrophilic behavior, typical of most lignocellulosic fillers. As indicated by Vogler [32], surfaces with a contact angle of less than 65º have a hydrophilic character, this being a typical behavior of biofillers, due to the large number of hydroxyl groups (-OH) present in their structure [33]. Regarding the evolution of the contact angle of PPF after silanization with GLYMO, it is worthy to note that it rapidly decreases in a similar way to untreated PPF during the first 30 s; after this time the decrease is less pronounced, reaching a constant value of 50º.

These results suggest that some of the hydroxyl groups available in PPF have reacted with the hydrolyzed alkoxysilane, thus reducing the affinity of PPF to water absorption [24]. This phenomenon has been observed by several studies by using FTIR characterization. In particular, the intensity of the band corresponding to the hydroxyl groups of cellulose (3200 cm^{-1}) decreases, while a new peak located at 1200 cm^{-1} can be detected, which is attributed to Si-O-Si vibration. Moreover, the appearance of a peak at 800 cm^{-1} corresponding to Si-OH which is attributed to the reaction between the silanol groups (Si-OH), and the hydroxyl groups (-OH) of cellulose, thus confirming the condensation between them, which proves the anchoring of the hydrolized alkoxysilane into the outmost layer of the lignocellulosic particles [30, 34, 35]. The PPF treated with palmitoyl chloride exhibits practically unchanged contact angle values during the 120 s of measurement (128.6º), thus demonstrating the high efficiency of the treatment in providing a high hydrophobic behaviour to the PPF (contact angle > 65º). In fact, it can be considered a superhydrophobic behaviour since the water contact angle is even greater than 150º.

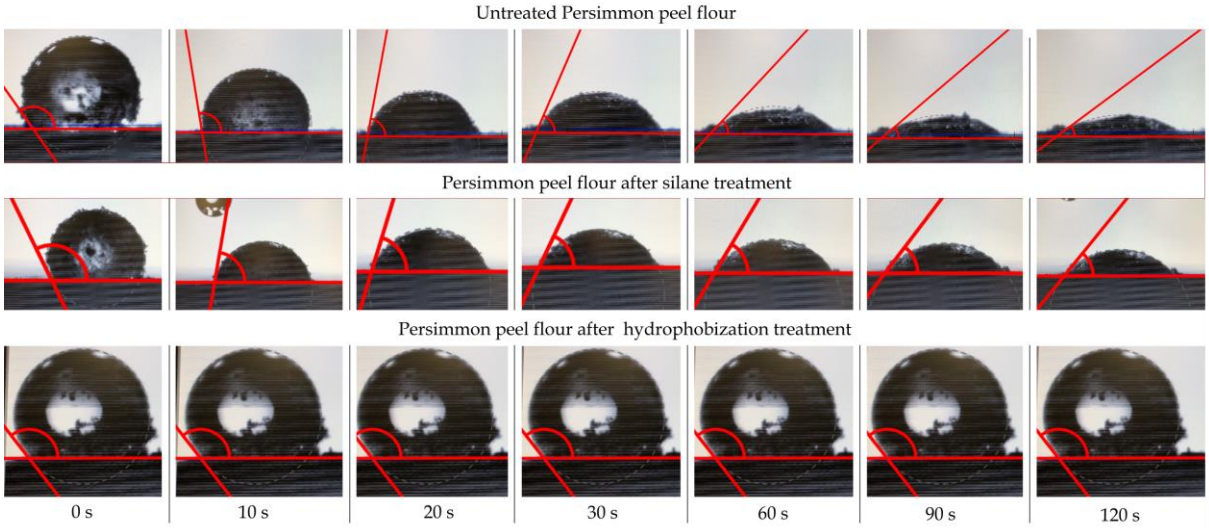

Figure 3. Comparative plots of the evolution of the dynamic water contact angle of untreated persimmon peel flour (upper row), persimmon peel flour after silanization with GLYMO treatment (middle row), and persimmon peel flour after hydrophobization with palmitoyl chloride (bottom row).

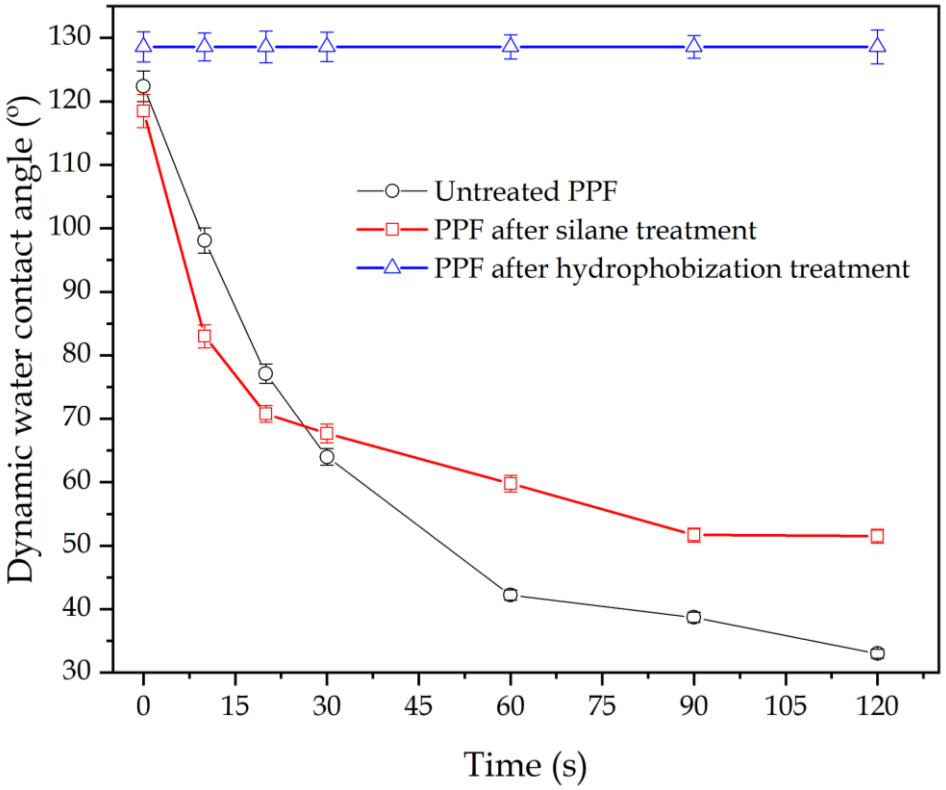

Figure 4. Variation of the dynamic water contact angle of persimmon peel flour as a function of time with different treatments: untreated, after silanization with GLYMO, and after hydrophobization with palmitoyl chloride.

3.1.2. Particle size and aggregation

To study the morphology and aggregate formation of PPF particles after both surface treatments, the washed and dried particles were observed by FESEM (**Figure 5**). **Figure 5a** shows PPF-SI powder with a particle size ranging from 70 to 90 µm. In addition, these particles present irregular shapes with a very slight roughness, due to the anchorage of the silanes on the PPF surface. The effect of the palmitoyl chloride treatment is also evident since the PPF particles exhibit a rough surface, as shown in **Figure 5b**, due to the thin hydrophobic layer formed on their surface. The particle size is smaller, with an average particle size in the range of 50 – 70 µm, thus indicating a lower tendency to form particle aggregates, which has a positive effect on particle dispersion [36].

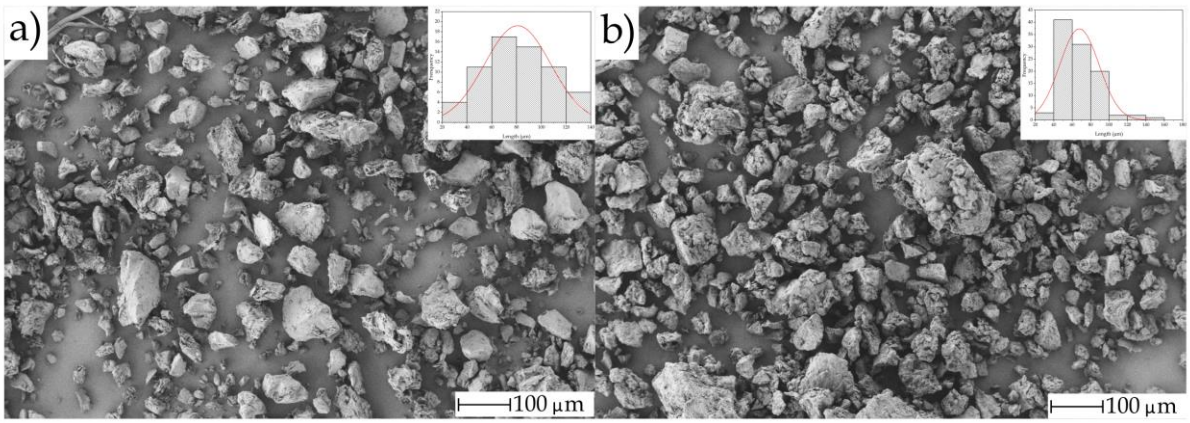

Figure 5. FESEM images of the persimmon peel flour after a) silanization with GLYMO, and b) hydrophobization with palmitoyl chloride. Images were taken at 100×, with a marker scale of 100 µm.

3.2. Characterization of Bio-HDPE/PPF composites

3.2.1. Mechanical Properties of Bio-HDPE/PPF composites

The tensile mechanical properties (E, σ_t, ε_b), impact strength, and Shore D hardness of neat Bio-HDPE and Bio-HDPE/PPF composites are gathered in **Table 1**. Regarding the tensile tests, it can be observed that the addition of PPF leads to a significant decrease in the percentage of elongation at break (%ε_b) from 609.7% for neat Bio-HDPE to approximately 10% for the Bio-HDPE/PPF composites without any compatibilization strategy, as well as a slight decrease in the Young's modulus (E) and the tensile strength (σ_t), reducing the typical ductile behaviour of HDPE [37]. This effect can be attributed to the fact that, due to the highly hydrophilic nature of untreated PPF and the hydrophobic nature of the HDPE matrix, a low affinity occurs, which makes the interaction between them relatively low, leading to a reduction in their tensile properties due to the stress concentration phenomenon [20]. As for Bio-HDPE/PPF composites, it can be observed that the different compatibilization strategies have a positive effect on the mechanical performance of Bio-HDPE/PPF composites. On the one hand, it can be seen that the treatments do not significantly affect the tensile strength, which remains practically unchanged for all samples. On the other hand, silane-treated PPF composites show a 10% and 20% increase in Young's modulus and elongation at break, respectively, compared to untreated PPF-filled composites. In addition, there is a 13% increase in the Young's modulus of the PE-*g*-MA compatibilized composite compared to the non-compatibilized sample (Bio-HDPE/PPF). This effect may be referred to the increased interaction between the PPF and the Bio- HDPE matrix since PE-*g*-MA can interact with both the polymer matrix (polyethylene

chain segments in PE-*g*-MA) and the lignocellulosic particle (due to the interactions between maleic anhydride and the hydroxyl groups in persimmon peel flour) [38, 39]. Improved interaction in Bio-HDPE/PPF-SI composites could be related to the reaction of the hydroxyl (-OH) groups present in PPF with the hydrolyzed silanol groups of GLYMO during silanization, as observed in other studies [24, 40]. Likewise, in the case of Bio-HDPE/PPF-MA, on one side, the reaction between maleic anhydride and the -OH groups of PPF, and on the other side, the PE segment chains in PE-*g*-MA, tend to interact with polyethylene chains of Bio-HDPE matrix, these two phenomena having a positive effect on increased interaction [41-43]. It should be noted that surface treatment with palmitoyl chloride enhances the hydrophobic nature of the PPF particles [36]. This has to two effects: firstly, it prevents aggregation of the particles, thus aiding a better particle dispersion into the Bio-HDPE polymer matrix [44], and secondly, a thin hydrophobic layer formed around the particles increases their compatibility with the Bio-HDPE matrix (which is highly hydrophobic) [45], thus resulting in better interaction between the PPF surfaces and the Bio-HDPE matrix [46]. These results are consistent with those reported by Garcia-Garcia, Carbonell-Verdu [20] and Dominici, García García [26], in composites of biobased polyethylene and spent coffee ground wastes, where the hydrophobic nature of the coffee waste was enhanced by palmitoyl acid-based treatments.

Table 1. Summary of the mechanical properties (tensile properties, Shore-D hardness and impact strength) of the neat Bio-HDPE and Bio-HDPE/PPF composites.

Code	E (MPa)	σ_t (MPa)	ε_b (%)	Impact Strength (kJ/m²)	Shore D hardness
Bio-HDPE	201.3 ± 6.5	21.6 ± 0.3	609.7 ± 38.1	4.8 ± 0.3	56.6 ± 0.9
Bio-HDPE/PPF	187.2 ± 9.5	15.0 ± 0.8	10.0 ± 0.7	2.0 ± 0.1	60.4 ± 0.9
Bio-HDPE/PPF-SI	224.5 ± 8.7	16.9 ± 0.4	12.0 ± 0.4	2.6 ± 0.3	57.8 ± 0.8
Bio-HDPE/PPF-MA	227.0 ± 6.5	16.2 ± 0.3	9.8 ± 0.1	2.6 ± 0.5	60.0 ± 1.4
Bio-HDPE/PPF-PC	170.0 ± 7.9	17.4 ± 0.2	15.1 ± 0.7	3.1 ± 0.2	60.6 ± 0.5

The impact strength obtained in a Charpy test can be useful to assess improved toughness. It can be observed that the impact energy absorption capacity of Bio-HDPE is drastically reduced with the addition of untreated PPF (less than the half). As mentioned, the low interaction due to the incompatibility between highly hydrophilic PPF particles and the highly hydrophobic polyethylene matrix results in small gaps between the particles and the matrix, as well as microcracks [20]. Considering the PPF-reinforced samples, it can be observed that the different compatibilization strategies lead to an increase in the impact-absorbed energy compared to composites with untreated PPF filler and no other compatibilizer. This increase in

the absorbed-energy is due to the enhanced interaction between the biofiller and the surrounding polyethylene matrix, leading to a decrease in gap size, thus preventing microcrack growth. As can be seen, composites with hydrophobized PPF with palmitoyl chloride (Bio-HDPE/PPF-PC) offer the highest impact energy absorption of all composites in this study, with an impact strength of 3.1 kJ/m^2, which represents an increase of approximately 56% over composites with untreated PPF. This is due to the higher hydrophobicity of the PPF achieved with palmitoyl chloride, which results in better particle dispersion into the polyethylene matrix and better compatibility with the matrix, preventing crack formation and growth [44]. Finally, it can be observed that the addition of PPF in the Bio-HDPE matrix causes an increase in hardness, with an increase of approximately 7% on the shore D scale with respect to neat Bio-HDPE.

3.2.2. Morphology of Bio-HDPE/PPF composites

To study the effect of the different compatibilization strategies, the fractured surfaces of the impact-tested samples of neat Bio-HDPE and Bio-HDPE/PPF composites were observed by FESEM (see **Figure 6**). **Figure 6a** shows the fracture corresponding to the neat Bio-HDPE sample, which presents a rough and irregular surface, marked by the presence of valleys and peaks, which is consistent with a ductile fracture typical of HDPE [37]. The addition of PPF clearly causes a disruption in the Bio-HDPE matrix, observed with the presence of large gaps between the PPF particles and the surrounding matrix, as indicated by the red arrows in **Figure 6b**, thus revealing a low interaction as mentioned above due to the different hydrophobic nature of both components. This makes the different deformation capacity of the filler and the matrix more noticeable [47], causing a mixed fracture type, where a ductile-type fracture is observed for the matrix and a pull-off phenomenon for PPF particles can also be detected. As shown in **Figure 6c and 6d,** both the use GLYMO-silanized PPF particles, and the use of PE-*g*-MA compatibilizer in composites, increase the interfacial interaction between the matrix and the filler, resulting in a noticeable decrease in the gaps between PPF particles and the surrounding matrix, as indicated by the green circles. These morphologies are responsible for improved mechanical properties, with a slight increase in tensile strength and, mainly, in impact-absorbed energy. Finally, it can be observed that the composites materials with hydrophobized PPF particles with palmitoyl chloride also offer a clear decrease in the size of the gap between the embedded PPF particles and the polyethylene matrix (F**igure 6e**), which is a clear evidence of improved compatibility between them due to a marked increase in the hydrophobic nature of the PPF. Moreover, this increase in hydrophobicity is also responsible for lower aggregate

formation, as seen previously, thus improving their distribution in the polymer matrix, as indicated by the blue arrows.

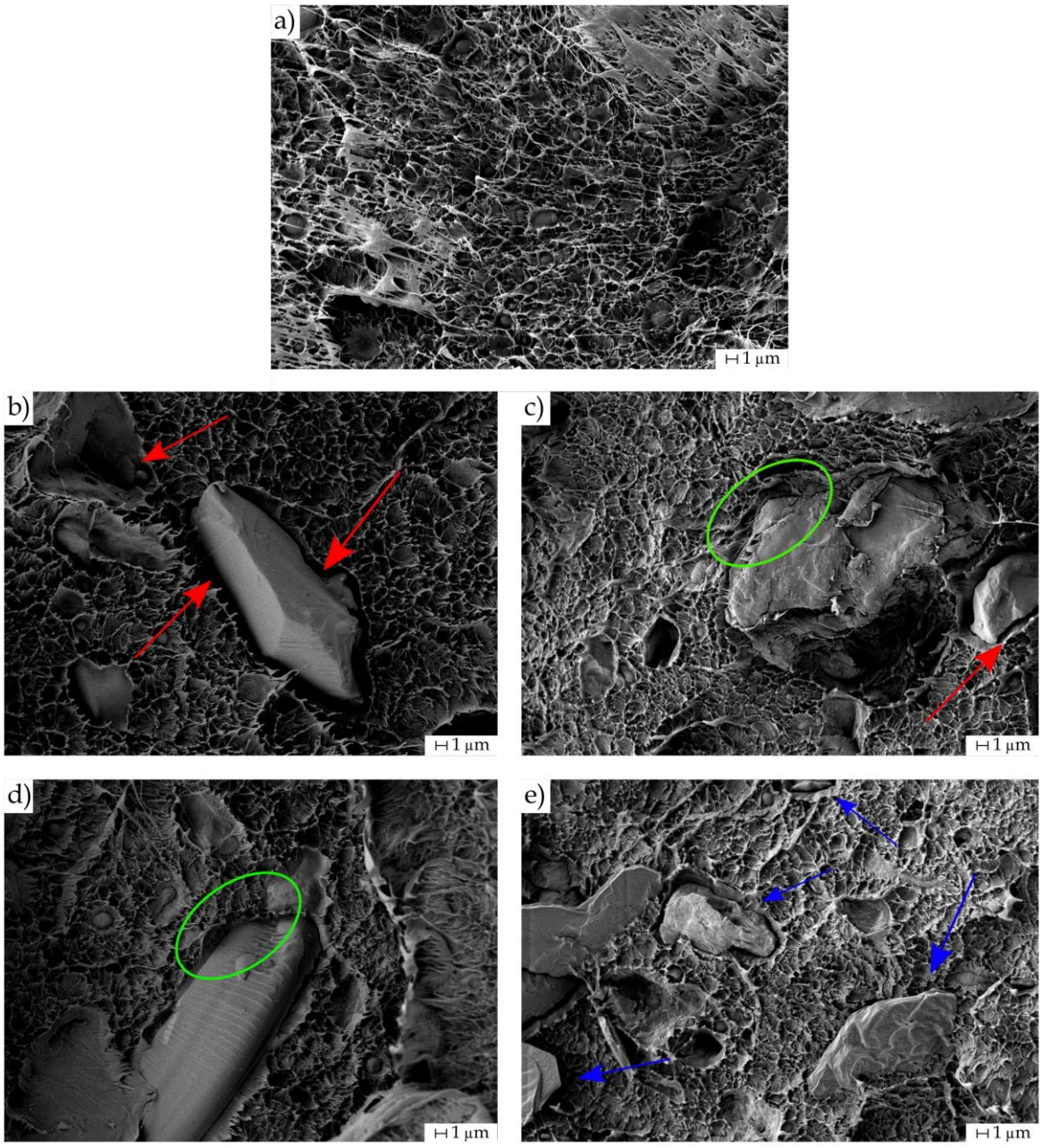

Figure 6. FESEM images of the fracture surfaces of a) Bio-HDPE, b) Bio-HDPE/PPF, c) Bio-HDPE/PPF-SI, d) Bio-HDPE/PPF-MA, and e) Bio-HDPE/PPF-PC. Images were taken at 2500×, with a marker scale of 1 µm

3.2.3. Thermal properties of Bio-HDPE/PPF composites

Figure 7 displays the calorimetric curves obtained from the DSC (dynamic) runs. **Figures 7a and 7b** correspond to the cooling step and the second heating step, respectively. These were used to calculate the crystallization peak temperature (T_c), the melting peak temperature (T_m)

and the melting enthalpy (ΔH_m). As can be seen, the addition of PPF in the Bio-HDPE matrix hardly affects its crystallization and its characteristic melting peak temperature, obtaining in all reinforced samples very similar temperatures, around 116 ºC and 130 ºC, respectively, in accordance with the typical crystallization and melting of HDPE [48].

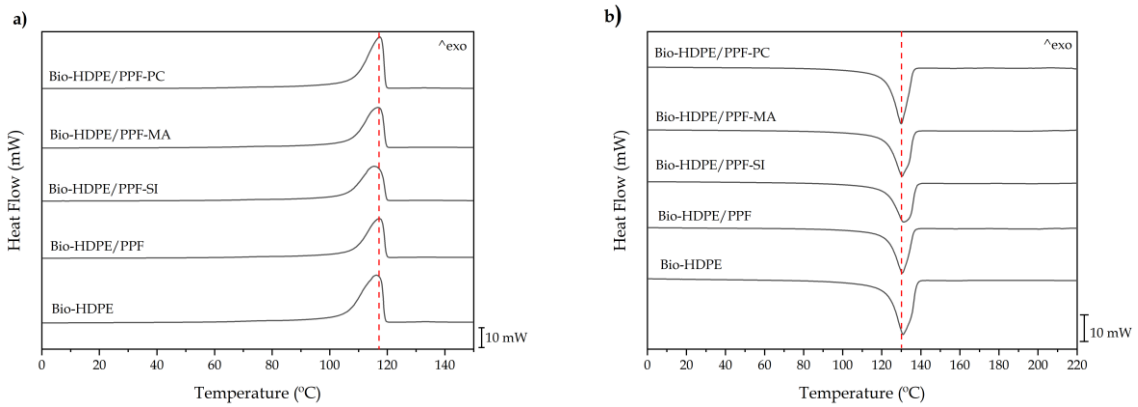

Figure 7. DSC curves of Bio-HDPE, and Bio-HDPE/PPF composites a) cooling step, b) 2nd heating step.

Concerning crystallinity (**Table 2**), it can be seen how the addition of PPF in the Bio-HDPE matrix causes a decrease in the degree of crystallinity down to 66%, remaining practically constant in Bio-HDPE/PPF composites with silane-treated PPF and in the composites compatibilized with PE-*g*-MA ($X_c \approx 66\%$). However, it can be observed that the addition of hydrophobized PFF with palmitoyl chloride leads to an increase in crystallinity up to 74%. This increase is due to the fact that the smaller particle size and a better dispersion can exert a nucleating effect that contributes to increase the degree of crystallinity of the Bio-HDPE matrix [49].

Table 2. Summary of thermal parameters obtained by DSC curves of neat Bio-HDPE and Bio-HDPE/PPF composites.

Code	T_c (°C)	T_m (°C)	ΔH_m (J/g)	X_c (%)
Bio-HDPE	116.2 ± 2.3	130.9 ± 2.4	206.8 ± 3.8	70.6 ± 1.3
Bio-HDPE/PPF	117.2 ± 2.1	130.9 ± 2.0	156.2 ± 2.7	66.6 ± 1.5
Bio-HDPE/PPF-SI	115.6 ± 2.1	131.3 ± 2.0	155.2 ± 2.3	66.2 ± 1.3
Bio-HDPE/PPF-MA	116.7 ± 2.5	130.4 ± 2.7	154.7 ± 3.3	66.0 ± 1.3
Bio-HDPE/PPF-PC	117.3 ± 2.5	129.9 ± 2.7	174.5 ± 3.7	74.4 ± 1.5

The stabilization effect of PPF biofiller on Bio-HDPE/PPF composites was assessed by isothermal DSC. **Figure 8** shows the DSC curves corresponding to the isothermal DSC runs at 210 ºC of different Bio-HDPE/PPF composites to determine the oxidation stability over time. Bearing in mind that all the composites have undergone melting process of Bio-HDPE matrix, it can be observed that the time at which the oxidation process occurs differs for the different samples. The oxidation induction time (OIT) was determined under isothermal conditions in air atmosphere at 210 °C. At this temperature, Bio-HDPE can undergo oxidation due to processing temperatures, UV light, oxidant atmosphere, and so on [50]. The OIT can be identified by the onset of an exothermic peak, related to thermo-oxidation. As expected, degradation of unfilled Bio-HDPE occurs shortly after reaching 210 °C (OIT ≈ 4.8 min). The effect of the addition of PPF into the Bio-HDPE matrix is remarkable and positive in terms of thermal stabilization. This is directly related to the large amount of phenolic compounds (caffeic, *p*-coumaric, ferulic and gallic acids) as well as other antioxidant compounds such as proanthocyanidins, which reduce the oxidative effect by free radical scavenging [51, 52]. The total number of hydroxyl groups could significantly affect their antioxidant activity due to their reactivity [53]. Such compounds, in the case of untreated PPF, are readily available to provide antioxidant properties to the Bio-HDPE matrix as they are in direct contact with it, causing the OIT to be delayed by approximately 43 min, thus achieving a noticeable stabilization effect compared to neat Bio-HDPE. However, it is worthy to highlight two different behaviours: composites containing hydrophobized PPF particles with palmitoyl chloride (Bio-HDPE/PPF-PC) and composites with silanized PPF particles with GLYMO (Bio-HDPE/PPF-SI). In the first case, it can be observed that the PPF-reinforced sample treated with palmitoyl chloride shows a premature degradation, with an OIT of 5.7 minutes, only 1 minute above that of neat Bio-HDPE. This is due to the fact that the thin hydrophobic layer that covers the PPF particles prevents the transfer of the antioxidant compounds from PPF to the Bio HDPE matrix, leading to poor stabilization properties. On the other hand, composites with silanized GLYMO+PPF particles show a great improvement in OIT, bringing the degradation of the Bio-HDPE/PPF-SI composite to 82.5 min. This may be due to the strong interaction generated between the functional organic silane with the polyethylene chains and the antioxidants (phenols) of the PPF [54], producing a higher retention of these antioxidants in the HDPE matrix and, as a consequence, an improvement in OIT, as proposed by Albarino and Schonhorn [55], [56]. These results are consistent with those obtained by Quiles-Carrillo, Montava-Jordà [57], who achieved delays in OIT of 56 min and 240 min in an HDPE matrix by adding natural antioxidants, namely 0.3 and 0.8 phr of gallic acid. They showed even better results than those obtained by Kabir, Li [58] when using a commercial

antioxidant such as Irganox® 1010, which delayed the OIT of LDPE from 2 min to 35.9 min. These results demonstrate the high value of persimmon wastes (peels) as a source of antioxidant compounds of natural origin, which can be used in food sectors, as well as being a viable alternative to replace synthetic antioxidants used to reduce the oxidation induction time of PE and other polyolefins [59, 60].

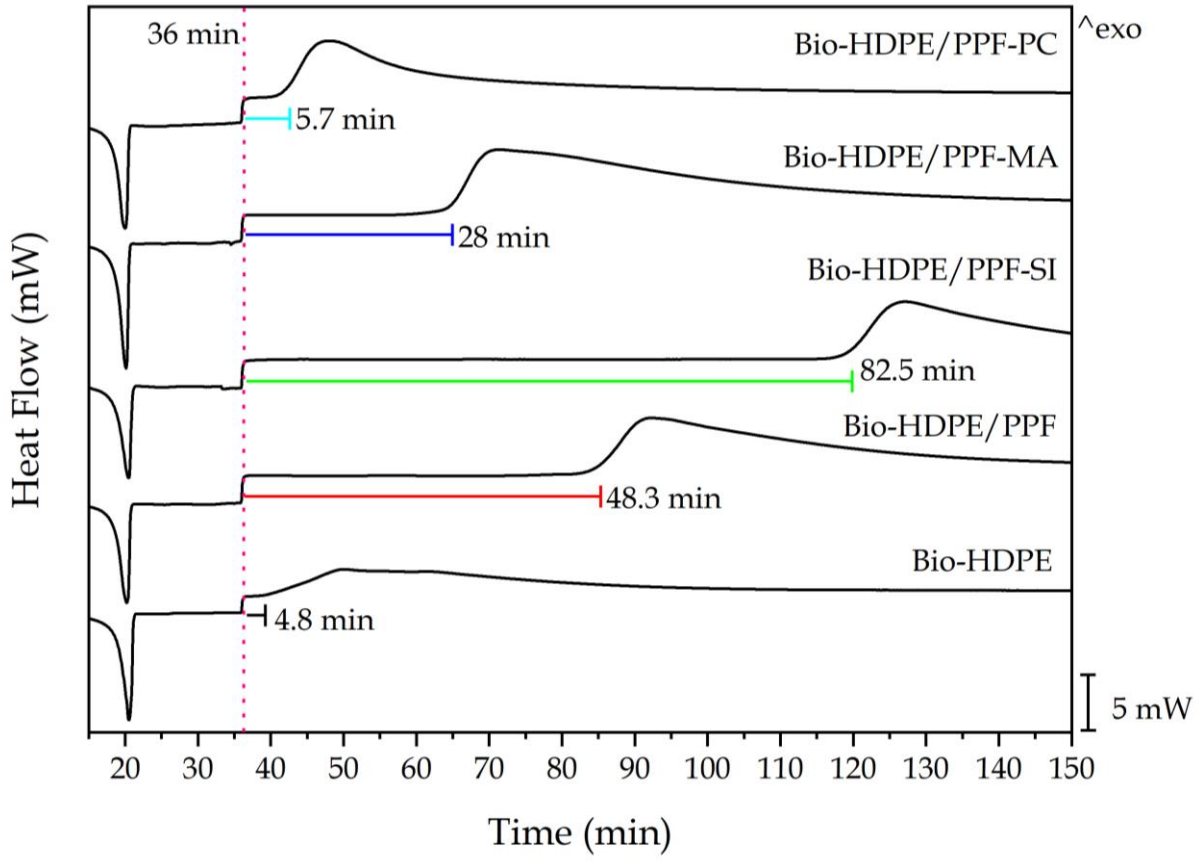

Figure 8. DSC isothermal curves at 210 ºC of Bio-HDPE, and Bio-HDPE/PPF composites.

In addition, the thermal stability at high temperatures was also studied. **Figure 9** gathers the thermograms obtained by TGA analysis. The main thermal degradation parameters obtained from TGA are shown in **Table 3**. As can be seen, neat Bio-HDPE undergoes thermal degradation in a single-step process, with a degradation onset temperature (T_{onset}) of 345.3 ºC, and a maximum degradation rate temperature of 450.8 ºC, which generally corresponds to the degradation of carbon atoms, according to the literature [20]. The thermal degradation of persimmon peel flour is in accordance with the typical degradation profile of a lignocellulosic filler, characterized by three main steps. The first step takes place at 110 °C with a mass loss of approximately 2.5 - 3% corresponding to the removal of residual moisture. The next stage

involves a mass loss of about 60%, which generally corresponds to the depolymerization of hemicellulose and cellulose, and the degradation of pectin, in the range of 220 ºC - 380 ºC. The third stage corresponds to the degradation of residual lignin up to 600 ºC [49]. However, it can be observed that the residual mass of the composites is relatively low and similar because both the Bio-HDPE matrix and the natural filler degrade completely at 700 ºC.

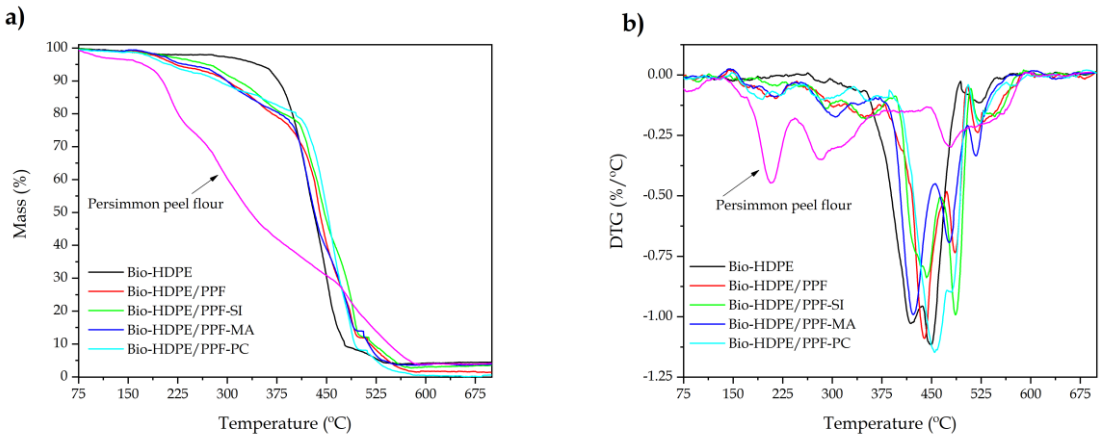

Figure 9. Comparative plots of a) thermogravimetric (TGA) curves and b) DGT curves of Bio-HDPE, Bio-HDPE/PPF composites, and persimmon peel flour.

As shown in **Figure 9a**, the addition of PPF in Bio-HDPE results in a remarkable reduction of the T_{onset} of Bio-HDPE/PPF composites, lowering the temperature largely from 345.3 ºC (Bio-HDPE) to 221.3 ºC (Bio-HDPE/PPF), this effect can be attributed to the poor stability of lignocellulosic fillers at low temperatures where premature degradation of organic compounds (hemicellulose) occurs [26], as shown in **Figure 9b**. Nevertheless, Bio HDPE-PPF composites with some coupling agent show a slight improvement in T_{onset}, the most noticeable being the sample containing silane-treated PPF with a temperature of 268.3 ºC (47 ºC higher than untreated PPF), approximately. These results are in agreement with those obtained by DSC. In addition, the maximum degradation rate temperature was delayed for all cases in Bio-HDPE/PPF composites compared to neat Bio-HDPE. This may be attributed to the presence of antioxidants from the polyphenolic compounds in PPF, suggesting that the greatest contribution of antioxidant compounds occurs at high temperatures. The delay is up to ≈ 36 ºC in the case of the silane-pretreated PPF (PPF-SI), where it is more noticeable due to the better retention of the antioxidant properties as a result of the enhanced interaction between the PPF particles and the HDPE matrix [55]. Although the use of PE-*g*-MA provides good interaction between the matrix and the filler, this is the composite with the lowest T_{deg}, about 10 ºC lower than PPF-SI. As suggested by Araújo, Waldman [61], the enhanced interaction obtained by the reaction of the

maleic anhydride groups of PE-*g*-MA with the (-OH) groups of PPF also enhances the interaction during the degradation process; as a result, when the HDPE degrades, it accelerates the degradation of PPF and, consequently, the resulting composite is also more sensitive to thermal degradation.

Table 3. Summary of thermal parameters obtained by TGA of the Bio-HDPE sample and Bio-HDPE/PPF composites.

Code	T_{onset} (°C)	T_{deg_1} (°C)	T_{deg_2} (°C)	Residual mass (%)
Bio-HDPE	345.3 ± 6.9	450.8 ± 9.0	-	4.5 ± 0.01
Bio-HDPE/PPF	221.3 ± 4.4	439.4 ± 8.8	485.4 ± 9.7	1.4 ± 0.01
Bio-HDPE/PPF-SI	268.3 ± 4.8	442.4 ± 8.9	486.4 ± 9.7	3.5 ± 0.02
Bio-HDPE/PPF-MA	237.3 ± 4.3	422.4 ± 9.3	476.3 ± 10.5	3.8 ± 0.02
Bio-HDPE/PPF-PC	212.8 ± 4.7	454.9 ± 6.8	479.4 ± 7.2	0.5 ± 0.01

3.2.4. Dynamic-mechanical characterization of Bio-HDPE/PPF composites

The dynamic-mechanical thermal analysis (DMTA) curves of neat Bio-HDPE and Bio-HDPE/PPF composites are shown in **Figure 10**. **Figure 10a** illustrates the effect of the addition of PPF in the Bio-HDPE matrix on the evolution of the storage modulus (*E'*) in the temperature range from -150 to 125 °C. In general, the storage modulus shows a marked tendency to decrease with increasing temperature. At low temperatures (-125 ºC) the behavior of Bio-HDPE/PPF composites with three compatibilization strategies is very similar to that of neat Bio-HDPE, exhibiting approximately *E'* values close to 2275 MPa (**Table 4**). This phenomenon can be attributed to a rather good polymer-particle interaction, which causes these particles to show a pseudo-lubricating effect that makes them slide more easily between the HDPE chains, resulting in more homogeneous composites [47]. It can also be observed that Bio-HDPE/PPF (untreated PPF) composites show a higher *E'* value (2592 MPa) compared to neat Bio-HDPE; this is related to the absence of compatibility between both components, as previously described in the FESEM characterization. The addition of untreated PPF causes a restriction of the mobility of the polyethylene chains due to the interference they have with the matrix, and as a consequence a higher stiffness is obtained [62]. As the temperature increases, a large decrease in *E'* values are observed. This transition at about -100 ºC is related to the glass to rubber transition region. This is mainly due to the softening of the HDPE matrix caused by the contribution of thermal energy to the chains, which favors their mobility [63]. At -50 ºC the Bio-HDPE/PPF composites show higher storage modulus values than neat Bio-HDPE with values close to 1438 MPa. As suggested by Sewda and Maiti [47], PE and biofiller expand and contract in a different

way due to their nature, resulting in an increase in the mobility restriction of the HDPE chains. By increasing the temperature above 50 °C, the storage modulus decreases markedly for all composites down to values of 500 MPa, which is related to the α-transition of low branched polyethylenes.

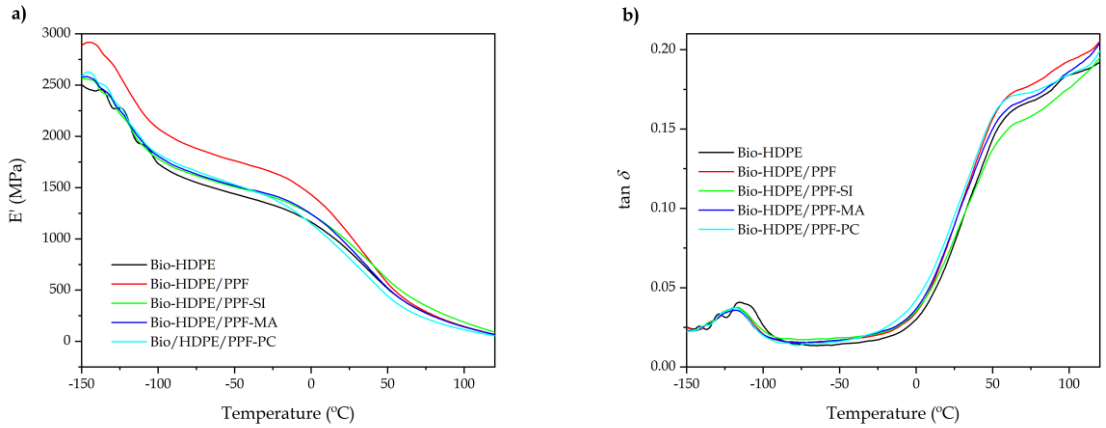

Figure 10. Comparative plots of the evolution of a) Storage modulus, and b) damping factor (tan δ) as a function of the temperature of the Bio-HDPE sample, and Bio- HDPE/PPF composites.

Figure 10b depicts the curves corresponding to the dynamic damping factor (tan δ) over a temperature range from -150 to 125 °C of neat Bio-HDPE and Bio-HDPE/PPF composites. High-density polyethylene typically exhibits two types of relaxations that are observed with temperature variation. The γ-relaxation that usually appears in the temperature range between -140 and -100 ºC, which is related to the motion of a small part of the chains in the amorphous region of the polymer, and is associated with the glass transition temperature (T_g) and the second relaxation, called α-relaxation, which occurs at temperatures between 0 ºC and 120 ºC, with a peak at 40-50 ºC, and is associated with the motion of the chains folds on the surface of the lamellae in the crystalline regions [47, 63]. It can be observed that Bio-HDPE presents a glass transition temperature (identified by the peak of the γ-transition) with a value of -115 ºC and the α-transition at a temperature of approximately 50 ºC, which are consistent with the results reported by Jorda-Reolid, Gomez-Caturla [64]. The addition of PPF leads to a small decrease in the glass transition temperature by about 3 °C, due to the increased interaction between the PPF particles and the matrix, as above-mentioned. A decrease in the intensity of the γ-relaxation peak can be observed due to the increased internal friction caused by the PPF, which restricts the movement of the polyethylene chains [13].

Table 4. Dynamic-mechanical thermal properties (DMTA) of neat Bio-HDPE, and Bio-HDPE/PPF composites in terms of storage modulus (*E'*) at different temperatures, and glass transition temperature (T_g).

Code	E′ at -125 °C (MPa)	E′ at -50 °C (MPa)	E′ at 50 °C (MPa)	T_g (°C)
Bio-HDPE	2275 ± 45	1439 ± 29	515 ± 10	-115.3 ±2.3
Bio-HDPE/PPF	2592 ± 52	1763 ± 35	570 ± 11	-118.1 ± 2.1
Bio-HDPE/PPF-SI	2221 ± 33	1509 ± 23	606 ± 12	-116.2 ± 2.1
Bio-HDPE/PPF-MA	2256 ± 34	1518 ± 23	522 ± 10	-118.1 ± 2.1
Bio-HDPE/PPF-PC	2295 ± 50	1530 ± 34	444 ± 10	-118.2 ± 2.0

3.2.5. Water uptake analysis

The water absorption of Bio-HDPE/PPF composites as a function of immersion time is shown in **Figure 11**. As can be seen, the water absorption of unfilled Bio-HDPE is practically negligible during the test period, due to its non-polar character and high hydrophobicity [65]. The addition of PPF has a clear impact on water absorption capacity, showing an increasing trend over time in all composites. This may be due to several factors, one of which is the existence of small voids and pores in the structure due to the lack of interaction between the matrix and the filler. The existence of these voids in the internal structure of the composite materials enables water to enter, thus increasing their water absorption [66]. Another factor is the hydrophilic nature of the biofillers, due to the large number of hydroxyl groups present in PPF, belonging to phenols, proanthocyanidins, condensed tannins and fiber content (cellulose, hemicellulose and lignin), which promote water absorption by hydrogen bonding [7, 67, 68]. This effect is evident after the first week of immersion, especially in composites containing untreated PPF. This may be related to the fact that the access to the available hydroxyl groups (-OH) is greater, thus enhancing the interaction with water. In spite of this, maximum water absorption values do not exceed 0.7% during the 9 weeks. It can be seen that composites compatibilized with PE-*g*-MA and composites with silanized PPF show a similar behavior, obtaining a remarkable decrease in water absorption, with asymptotic values of 0.45%. This is mainly due to the decrease in available hydroxyl groups (-OH), which hinders their interaction with water, causing the percentage of water saturation to decrease with respect to composites with untreated PPF. Bio-HDPE/PPF composites compatibilized with PE-*g*-MA show lower water uptake due to a higher polymer-particle interaction because of the possible reaction of maleic anhydride with some -OH groups of PPF [18]. On the other hand, during the silanization of PPF with GLYMO, the hydroxyl groups generated after the hydrolysis of the alkoxysilane can also react with some hydroxyl groups present in PPF [24]. Finally, it can be observed that composites with

hydrophobized PPF with palmitoyl chloride show the lowest water absorption after 9 weeks of immersion (0.3%). This can be attributed to the esterification reaction between the hydroxyl groups present in the PPF with palmitic acid, which gives the material a hydrophobic nature, as previously described by dynamic water contact angle [30, 69]. The hydrophobic nature of the high-density polyethylene matrix remains virtually invariable during long exposure to water.

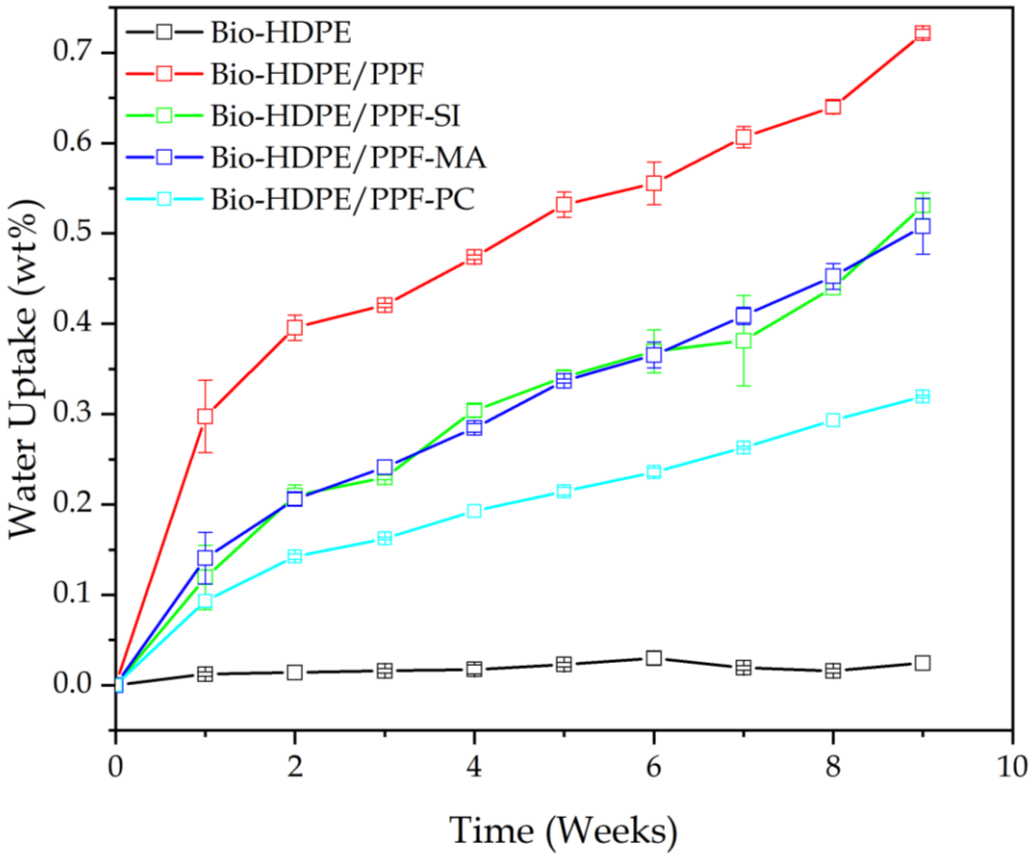

Figure 11. Evolution of the water uptake as a function of the immersion time of neat Bio-HDPE and BioHDPE/PPF composites.

3.2.6. Colorimetry Properties

Figure 12 shows the visual appearance of neat Bio HDPE and Bio-HDPE/PPF composites. It can be appreciated that the addition of PPF has a clear effect on the color change of the Bio-HDPE/PPF samples, shifting from a white tone characteristic of HDPE to a darker tone, due to the natural orange-red color of the persimmon peel flour provided by the amount of total carotenoids (*β*-cryptoxanthi, zeaxanthin, among others) and lycopene content [70, 71].

Figure 12. Visual appearance of the Bio HDPE sample and the Bio-HDPE/PPF composites.

The CIELab colour coordinates as well as the ΔE^* of the Bio-HDPE and Bio-HDPE/PPF composites are listed in **Table 5**. As previously mentioned, the colour change caused by the incorporation of PPF is noticeable, resulting in a significant decrease in lightness (L^* coordinate), as well as positive values for the a^* and b^* coordinates in all Bio-HDPE/PPF composites, compared to unfilled Bio-HDPE. It can also be observed that the different surface treatments on PPF have a slight effect on the final colour of the samples. In fact, Bio-HDPE/PPF-SI composite shows a lighter brown colour than the other composites, tending more to a yellowish (b^*) and reddish (a^*) appearance. This is probably due to the large number of antioxidant compounds in persimmon peel, which prevents the formation of quinones by interaction with oxygen, thus preventing the blackening of the compounds [72]. Interestingly, the treatment with palmitoyl chloride in PPF causes a slight darkening of the samples, since the hydrophobic layer around the particles slightly inhibits the antioxidant action, thus resulting in darker particles. Subsequently, the corresponding composites offer a surface appearance similar to dark woods such as oak wood [73]. This feature can be particularly attractive for some industrial sectors such as furniture, as the hydrophobic layer created around the particles can serve as a protective film, reducing the interaction with external agents such as oxygen, UV light and water, thus reducing surface deterioration over long exposure periods. As Nzokou,

689 Kamdem [74] suggests that the surface finish (varnish) of woods can cause both colour and
690 roughness to remain for more than 1000 and 450 h unchanged.

691 **Table 5.** Summary of the CIELAB color coordinates of the Bio-HDPE sample and the Bio-
692 HDPE/PPF composites.

	L*	a*	b*	ΔE*ab
Bio-HDPE	72.1 ± 1.1	-2.3 ± 0.0	-4.5 ± 0.1	-
Bio-HDPE/PPF	33.8 ± 0.6	2.1 ± 0.2	3.1 ± 0.3	39.3 ± 0.7
Bio-HDPE/PPF-SI	36.2 ± 1.1	4.3 ± 0.1	5.5 ± 0.2	37.9 ± 1.0
Bio-HDPE/PPF-MA	33.5 ± 0.7	1.6 ± 0.2	2.2 ± 0.3	39.4 ± 0.8
Bio-HDPE/PF-PC	32.1 ± 1.2	0.7 ± 0.1	1.2 ± 0.2	40.5 ± 1.2

693

694 *3.2.7. Antioxidant capacity of Bio-HDPE/PPF composites*

695 The antioxidant activity of persimmon peel is known to be provided by phenolic
696 compounds, including gallic acid, ferulic acid, caffeic acid and *p*-coumaric acid, as well as
697 carotenoids (β-carotene, and lycopene), and proanthocyanidins (condensed tannins) [7, 68, 75].
698 However, the amount of these compounds may vary due to factors such as fruit variety, climate,
699 cultivation, harvesting and storage processes [70, 76, 77]. The study of antioxidant activity was
700 based on the reduction of DPPH by electron transfer, which was measured by UV-Vis
701 spectroscopy, where an increase in antioxidant activity was observed by a color change from
702 violet to yellow [78]. **Figure 13** shows the DPPH radical scavenging activity of Bio-HDPE
703 samples and Bio-HDPE/PPF composites with respect to time (1 week). As suggested by Rojas-
704 Lema, Torres-Giner [79], in high-density polyethylene composites, the DPPH• radical can be
705 stabilized by the phenolic groups contained in the natural compounds to its non-radical form
706 DPPH-H. It can be noticed that after only one day (24 h) the absorbance of the composites with
707 MA and with silanized and hydrophobized PPF practically stabilizes, obtaining values of 89,
708 83 and 92%, respectively. Inferring that the hydroxyl groups available in PPF almost
709 completely reduce DPPH radicals. Although the PPF content remains constant for all Bio-
710 HDPE derived composites, the antioxidant activity is slightly affected by the compatibilizing
711 strategy. This effect is particularly noticeable in the composites with PPF treated with silanes,
712 where a retarding effect on the release of the antioxidant compounds is observed, stabilizing at
713 72 h with values close to 76%. This could be related to the fact that hydrolyzed silanols may
714 rearrange the geometry of the available hydroxyl groups, leading to electron delocalization,
715 which can affect the antioxidant activity (slowing and/or decreasing it) [80].

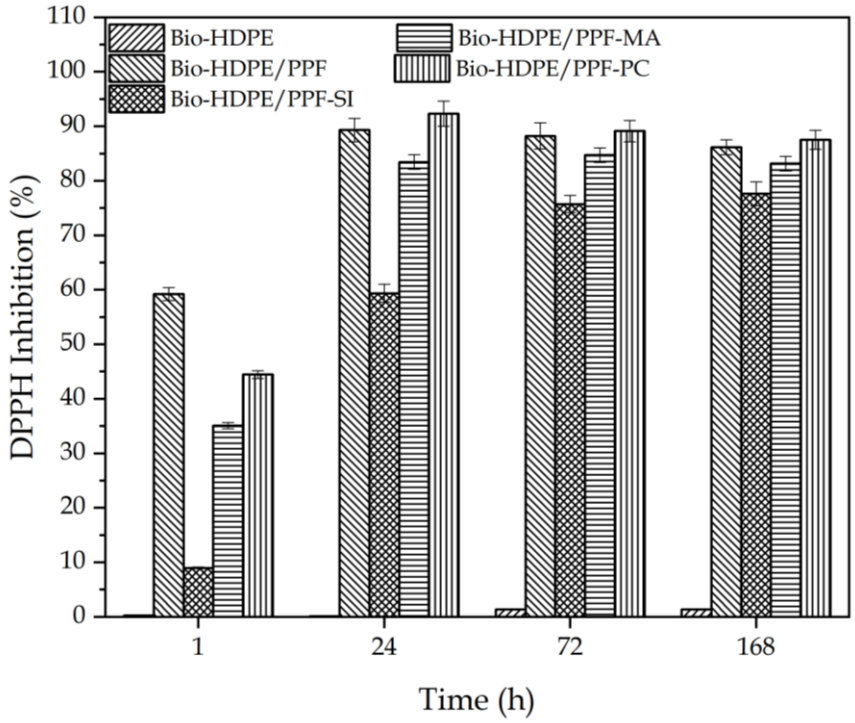

716

717 **Figure 13.** Percentage of 2,2-diphenyl-1-picrylhydrazyl radical (DPPH) inhibition of neat Bio-
718 HDPE and Bio-HDPE/PPF composites.

719

720 **4. Conclusions.**

721 Persimmon peel flour (PPF) waste is an interesting biofiller for Bio-HDPE-based
722 composites, that can be processed by injection molding. The effect of different
723 compatibilization strategies to enhance the interaction between the highly hydrophobic particles
724 and the highly hydrophobic Bio-HDPE matrix has been assessed. Overall, it was found that the
725 addition of PPF in the Bio-HDPE matrix resulted in a reduction of both tensile strength and
726 elongation at break due to stress concentration phenomena. These effects were clearly
727 diminished by using different compatibilization strategies: the use of a conventional PE-*g*-MA
728 copolymer during compounding, and a second strategy focused on a selective surface treatment
729 of PPF. The efficiency of two different surface treatments on PPF were studied: one silanization
730 process with GLYMO, and a hydrophobizing treatment with palmitoyl chloride. All three
731 strategies contribute to reduce the gap between the PPF particles and the surrounding Bio-
732 HDPE matrix, thus leading to more cohesion. A marked improvement in absorbed energy after
733 impact was observed in PPF-composites hydrophobized with palmitoyl chloride, leading to an
734 increase in the elongation at break, due to both improved particle dispersion in the matrix and
735 improved particle compatibility with each other. The water absorption capacity was

significantly reduced compared to composites with untreated PPF particles. These results are of great value considering that one of the weaknesses of composites of natural origin is their high sensitivity to water absorption, which causes changes in their dimensions when exposed to humid environments. The benefits of using persimmon fruit wastes as a source of natural antioxidants were clearly evidenced, obtaining a high inhibition of DPPH radicals, as well as delaying the oxidation induction time of the Bio-HDPE matrix. Therefore, the use of persimmon peel waste is an interesting approach to new wood-like composite materials with improved thermal stability. On the other hand, the hydrophobic surface treatment of PPF has demonstrated a clear advantage, as water uptake is significantly reduced.

Acknowledgments: Authors want to thank the Spanish Ministry of Science and Innovation, grant number MEN PID2020-116496RB-C22 for funding this research. D. Lascano wants to thank UPV for the grant received though the PAID-01-18 program. S. Rojas-Lema is a recipient of a Santiago Grisolia grant from Generalitat Valenciana (GVA) (GRISOLIAP/2019/132). J. Gomez-Caturla wants to thank Universitat Politècnica de València for his FPI grant from (SP20200080) J. Ivorra-Martinez thanks the Spanish Ministry of Science, Innovation and Universities for his FPU grant (FPU19/01759). Microscopy services at UPV are acknowledged for their help in collecting and analyzing FESEM images.

References

[1] M. C. López-Marcos, C. Bailina, M. Viuda-Martos, J. A. Pérez-Alvarez, J. Fernández-López, *Food and Bioprocess Technology* **2015**, *8*, 2400.

[2] R. H. Liu, *The American journal of clinical nutrition* **2003**, *78*, 517S.

[3] D. W. Wilson, P. Nash, H. S. Buttar, K. Griffiths, R. Singh, F. De Meester, R. Horiuchi, T. Takahashi, *Antioxidants* **2017**, *6*, 81.

[4] J. Boyer, R. H. Liu, *Nutrition journal* **2004**, *3*, 1.

[5] F. a. A. O. C. S. (FAOSTAT), "Production share of Persimmons by region", 2021, p. 2021/.

[6] R. Lucas-González, M. Viuda-Martos, J. A. P. Álvarez, J. Fernández-López, *Food chemistry* **2018**, *256*, 252.

[7] J. R. V. Matheus, C. J. d. Andrade, R. F. Miyahira, A. E. C. Fai, *Food Reviews International* **2020**, 1.

[8] S. Gea-Botella, L. Agulló, N. Martí, M. Martínez-Madrid, V. Lizama, F. Martín-Bermudo, G. Berná, D. Saura, M. Valero, *Food Research International* **2021**, *141*, 109882.

[9] A. Sharma, A. K. Dhiman, S. Attri, P. Ramachandran, *Journal of Food Processing and Preservation* **2021**, e15274.

[10] S. Karaman, Ö. S. Toker, F. Yüksel, M. Çam, A. Kayacier, M. Dogan, *Journal of Dairy Science* **2014**, *97*, 97.

[11] S. W. Kariuki, J. Wachira, M. Kawira, G. M. Leonard, *Advances in Materials Science and Engineering* **2019**, *2019*.

[12] L. Quiles-Carrillo, R. Balart, T. Boronat, S. Torres-Giner, D. Puglia, F. Dominici, L. Torre, *Fibers and Polymers* **2021**, 1.

[13] F. Burgada, E. Fages, L. Quiles-Carrillo, D. Lascano, J. Ivorra-Martinez, M. P. Arrieta, O. Fenollar, *Polymers* **2021**, *13*, 1248.

[14] PlasticsEurope, "Plastics- the Facts 2020: An analysis of European plastics production, demand and waste data", PlasticsEurope, Belgium, Europe, 2020.

[15] R. P. Babu, K. O'connor, R. Seeram, *Progress in biomaterials* **2013**, *2*, 1.

[16] A. Morschbacker, *Journal of Macromolecular Science®, Part C: Polymer Reviews* **2009**, *49*, 79.

[17] E. M. Fernandes, J. F. Mano, R. L. Reis, *Polyethylene-Based Blends, Composites and Nanocomposites* **2015**, 117.
[18] H. Gao, Y. Xie, R. Ou, Q. Wang, *Composites Part A: Applied Science and Manufacturing* **2012**, *43*, 150.
[19] A. A. Ramachandran, L. P. Mathew, S. Thomas, *European Polymer Journal* **2019**, *118*, 595.
[20] D. Garcia-Garcia, A. Carbonell-Verdu, A. Jordá-Vilaplana, R. Balart, D. Garcia-Sanoguera, *Journal of Applied Polymer Science* **2016**, *133*.
[21] B. Ferrero, V. Fombuena, O. Fenollar, T. Boronat, R. Balart, *Polymer Composites* **2015**, *36*, 1378.
[22] S. Chen, M. Yang, Y. Han, H. Liu, H. Zou, *European Polymer Journal* **2021**, *142*, 110114.
[23] H. Ismail, S. Shuhelmy, M. Edyham, *European Polymer Journal* **2002**, *38*, 39.
[24] Á. Agüero, D. Garcia-Sanoguera, D. Lascano, S. Rojas-Lema, J. Ivorra-Martinez, O. Fenollar, S. Torres-Giner, *Polymers* **2020**, *12*, 821.
[25] O. Bijaisoradat, L. Yue, I. Manas-Zloczower, H. Manuspiya, *Journal of Applied Polymer Science* **2021**, *138*, 50197.
[26] F. Dominici, D. García García, V. Fombuena, F. Luzi, D. Puglia, L. Torre, R. Balart, *Molecules* **2019**, *24*, 3113.
[27] S. Gorinstein, Z. Zachwieja, M. Folta, H. Barton, J. Piotrowicz, M. Zemser, M. Weisz, S. Trakhtenberg, O. Màrtín-Belloso, *Journal of agricultural and food chemistry* **2001**, *49*, 952.
[28] L. Quiles-Carrillo, T. Boronat, N. Montanes, R. Balart, S. Torres-Giner, *Polymer Testing* **2019**, *77*, 105875.
[29] E. Rojo, M. V. Alonso, B. Del Saz-Orozco, M. Oliet, F. Rodriguez, *Journal of Applied Polymer Science* **2015**, *132*.
[30] D. García-García, A. Carbonell, M. Samper, D. García-Sanoguera, R. Balart, *Composites part B: engineering* **2015**, *78*, 256.
[31] K.-H. Choi, K. S. Lee, J. H. Lee, J.-Y. Ryu, *Carbohydrate Polymers* **2020**, *246*, 116487.
[32] E. A. Vogler, *Advances in colloid and interface science* **1998**, *74*, 69.
[33] R. Martínez-Las Heras, E. Landines, A. Heredia, M. Castelló, A. Andrés, *Journal of food science and technology* **2017**, *54*, 2902.
[34] T. Lu, S. Liu, M. Jiang, X. Xu, Y. Wang, Z. Wang, J. Gou, D. Hui, Z. Zhou, *Composites Part B: Engineering* **2014**, *62*, 191.
[35] S. Qian, K. Sheng, *Composites Science and Technology* **2017**, *148*, 59.
[36] J. Xu, J. Xu, Y. Cao, X. Ji, Y. Yan, *Applied Surface Science* **2013**, *286*, 220.
[37] O. Daramola, A. Taiwo, I. Oladele, J. Olajide, S. Adeleke, B. Adewuyi, E. Sadiku, *Materials Today: Proceedings* **2021**, *38*, 682.
[38] H. Nitz, P. Reichert, H. Römling, R. Mülhaupt, *Macromolecular Materials and engineering* **2000**, *276*, 51.
[39] A. C. Wibowo, S. M. Desai, A. K. Mohanty, L. T. Drzal, M. Misra, *Macromolecular Materials and Engineering* **2006**, *291*, 90.
[40] I. C. Cabrera, S. Berlioz, A. Fahs, G. Louarn, P. Carriere, *International Journal of Biological Macromolecules* **2020**, *165*, 1773.
[41] S. Sahi, H. Djidjelli, A. Boukerrou, *Materials Today: Proceedings* **2021**, *36*, 67.
[42] H. Salmah, A. Azieyanti, *Journal of reinforced plastics and composites* **2011**, *30*, 195.
[43] H.-S. Kim, B.-H. Lee, S.-W. Choi, S. Kim, H.-J. Kim, *Composites Part A: Applied Science and Manufacturing* **2007**, *38*, 1473.
[44] Z. Qu, Q. Yu, *Construction and Building Materials* **2018**, *191*, 176.
[45] W. Liu, Z. Xie, X. Yang, Y. Wu, C. Jia, T. Bo, L. Wang, *Journal of the American Ceramic Society* **2011**, *94*, 1327.
[46] Z. Cao, M. Daly, L. M. Geever, I. Major, C. L. Higginbotham, D. M. Devine, *Composites Part B: Engineering* **2016**, *94*, 312.
[47] K. Sewda, S. Maiti, *Journal of applied polymer science* **2007**, *105*, 2598.

[48] Q. Zhang, M. U. Khan, X. Lin, H. Cai, H. Lei, *Composites part b: engineering* **2019**, *175*, 107151.
[49] Á. Agüero, D. Lascano, D. Garcia-Sanoguera, O. Fenollar, S. Torres-Giner, *Sustainability* **2020**, *12*, 652.
[50] L. Quiles-Carrillo, N. Montanes, V. Fombuena, R. Balart, S. Torres-Giner, *Polymer International* **2020**, *69*, 61.
[51] I. Kriston, Á. Orbán-Mester, G. Nagy, P. Staniek, E. Földes, B. Pukánszky, *Polymer Degradation and Stability* **2009**, *94*, 1448.
[52] P.-M. Li, G.-R. Du, F.-W. Ma, *Scientia horticulturae* **2011**, *129*, 710.
[53] P.-G. Pietta, *Journal of natural products* **2000**, *63*, 1035.
[54] Q. Pan, B. Wang, Z. Chen, J. Zhao, *Materials & Design* **2013**, *50*, 558.
[55] R. Albarino, H. Schonhorn, *Journal of Applied Polymer Science* **1973**, *17*, 3323.
[56] R. Albarino, H. Schonhorn, *Journal of Applied Polymer Science* **1974**, *18*, 635.
[57] L. Quiles-Carrillo, S. Montava-Jordà, T. Boronat, C. Sammon, R. Balart, S. Torres-Giner, *Polymers* **2020**, *12*, 31.
[58] A. S. Kabir, H. Li, H. Yuan, T. Kuboki, C. C. Xu, *Journal of Analytical and Applied Pyrolysis* **2019**, *140*, 413.
[59] A. Sanches-Silva, D. Costa, T. G. Albuquerque, G. G. Buonocore, F. Ramos, M. C. Castilho, A. V. Machado, H. S. Costa, *Food Additives & Contaminants: Part A* **2014**, *31*, 374.
[60] W. Yu, T. Reitberger, T. Hjertberg, J. Oderkerk, F. Costa, V. Englund, U. W. Gedde, *Polymer degradation and stability* **2015**, *111*, 1.
[61] J. Araújo, W. Waldman, M. De Paoli, *Polymer degradation and stability* **2008**, *93*, 1770.
[62] N. Montanes, D. Garcia-Sanoguera, V. Segui, O. Fenollar, T. Boronat, *Journal of Polymers and the Environment* **2018**, *26*, 1218.
[63] D. Castro, A. Ruvolo-Filho, E. Frollini, *Polymer Testing* **2012**, *31*, 880.
[64] M. Jorda-Reolid, J. Gomez-Caturla, J. Ivorra-Martinez, P. M. Stefani, S. Rojas-Lema, L. Quiles-Carrillo, *Polymers* **2021**, *13*, 922.
[65] S. K. Najafi, M. Tajvidi, M. Chaharmahli, *Journal of applied polymer science* **2006**, *102*, 3907.
[66] D. Lascano, D. Garcia-Garcia, S. Rojas-Lema, L. Quiles-Carrillo, R. Balart, T. Boronat, *Applied Sciences* **2020**, *10*, 3688.
[67] Y. Wen, C.-H. Tsou, C. Gao, J.-C. Chen, Z. Tang, Z. Chen, T. Yang, J. Du, Y. Yu, M.-C. Suen, *Journal of Polymer Research* **2020**, *27*, 1.
[68] C. Conesa, N. Laguarda-Miró, P. Fito, L. Seguí, *Waste and Biomass Valorization* **2019**, 1.
[69] Y. Zhang, Y. Xue, H. Toghiani, J. Zhang, C. U. Pittman, *Composite Interfaces* **2009**, *16*, 671.
[70] Y. Qi, X. Liu, Q. Zhang, H. Wu, D. Yan, Y. Liu, X. Zhu, X. Ren, Y. Yang, *Scientia Horticulturae* **2019**, *248*, 282.
[71] A. Salvador, L. Arnal, C. Besada, V. Larrea, A. Quiles, I. Pérez-Munuera, *Postharvest Biology and Technology* **2007**, *46*, 181.
[72] G. Lukmandaru, T. Ashitani, K. Takahashi, *Journal of Forestry Research* **2009**, *20*, 377.
[73] H. Turgut Sahin, M. Burak Arslan, S. Korkut, C. Sahin, *Color Research & Application* **2011**, *36*, 462.
[74] P. Nzokou, D. P. Kamdem, A. Temiz, *Progress in Organic Coatings* **2011**, *71*, 350.
[75] S. Yaqub, U. Farooq, A. Shafi, K. Akram, M. A. Murtaza, T. Kausar, F. Siddique, *Journal of Chemistry* **2016**, *2016*.
[76] L. Arnal, M. Del Río, *Food science and technology international* **2004**, *10*, 179.
[77] C. Besada, L. Arnal, A. Salvador, *Postharvest biology and technology* **2008**, *50*, 169.
[78] J.-H. Choe, H.-Y. Kim, Y.-J. Kim, E.-J. Yeo, C.-J. Kim, *International Journal of Food Properties* **2014**, *17*, 1779.
[79] S. Rojas-Lema, S. Torres-Giner, L. Quiles-Carrillo, J. Gomez-Caturla, D. Garcia-Garcia, R. Balart, *Antioxidants* **2021**, *10*, 14.
[80] E. Choe, D. B. Min, *Critical reviews in food science and nutrition* **2006**, *46*, 1.

860